AMERICAN SOCIETY FOR MICROBIOLOGY | mBio®

RESEARCH ARTICLE
Host-Microbe Biology

Simian Immunodeficiency Virus-Infected Memory CD4+ T Cells Infiltrate to the Site of Infected Macrophages in the Neuroparenchyma of a Chronic Macaque Model of Neurological Complications of AIDS

Cheri A. Lee,[a] Erin Beasley,[a] Karthikeyan Sundar,[a] Margery Smelkinson,[b] Carol Vinton,[c] Claire Deleage,[d] Kenta Matsuda,[a] Fan Wu,[a] Jake D. Estes,[e] Bernard A. P. Lafont,[f] Jason M. Brenchley,[c] Vanessa M. Hirsch[a]

[a]Laboratory of Molecular Microbiology, NIAID/NIH, Bethesda, Maryland, USA
[b]Biological Imaging, Research Technology Branch, NIAID/NIH, Bethesda, Maryland, USA
[c]Laboratory of Viral Diseases, NIAID/NIH, Bethesda, Maryland, USA
[d]AIDS and Cancer Virus Program, Frederick National Laboratory for Cancer Research, Frederick, Maryland, USA
[e]Vaccine and Gene Therapy Institute and Oregon National Primate Research Center (ONPRC), Oregon Health and Science University (OHSU), Beaverton, Oregon, USA
[f]Viral Immunology Section, Office of the Scientific Director, NIAID/NIH, Bethesda, Maryland, USA

ABSTRACT Simian immunodeficiency virus (SIV)-infected nonhuman primates can serve as a relevant model for AIDS neuropathogenesis. Current SIV-induced encephalitis (SIVE)/neurological complications of AIDS (neuroAIDS) models are generally associated with rapid progression to neuroAIDS, which does not reflect the tempo of neuroAIDS progression in humans. Recently, we isolated a neuropathogenic clone, SIVsm804E-CL757 (CL757), obtained from an SIV-infected rhesus macaque (RM). CL757 causes a more protracted progression to disease, inducing SIVE in 50% of inoculated animals, with high cerebral spinal fluid viral loads, multinucleated giant cells (MNGCs), and perivascular lymphocytic cuffing in the central nervous system (CNS). This latter finding is reminiscent of human immunodeficiency virus (HIV) encephalitis in humans but not generally observed in rapid progressor animals with neuroAIDS. Here, we studied which subsets of cells within the CNS were targeted by CL757 in animals with neurological symptoms of SIVE. Immunohistochemistry of brain sections demonstrated infiltration of CD4+ T cells (CD4) and macrophages (MΦs) to the site of MNGCs. Moreover, an increase in mononuclear cells isolated from the brain tissues of RMs with SIVE correlated with increased cerebrospinal fluid (CSF) viral load. Subset analysis showed a specific increase in brain CD4+ memory T cells (Br-mCD4), brain-MΦs (Br-MΦs), and brain B cells (Br-B cells). Both Br-mCD4s and Br-MΦs harbored replication-competent viral DNA, as demonstrated by virus isolation by coculture. However, only in animals exhibiting SIVE/neuroAIDS was virus isolated from Br-MΦs. These findings support the use of CL757 to study the pathogenesis of AIDS viruses in the central nervous system and indicate a previously unanticipated role of CD4s cells as a potential reservoir in the brain.

IMPORTANCE While the use of combination antiretroviral therapy effectively suppresses systemic viral replication in the body, neurocognitive disorders as a result of HIV infection of the central nervous system (CNS) remain a clinical problem. Therefore, the use of nonhuman primate models is necessary to study mechanisms of neuropathogenesis. The neurotropic, molecular clone SIVsm804E-CL757 (CL757) results in neuroAIDS in 50% of infected rhesus macaques approximately 1 year postinfection. Using CL757-infected macaques, we investigate disease progression by examining subsets of cells within the CNS that were targeted by CL757 and could potentially serve as viral reservoirs. By isolating mononuclear cells from the brains of

Citation Lee CA, Beasley E, Sundar K, Smelkinson M, Vinton C, Deleage C, Matsuda K, Wu F, Estes JD, Lafont BAP, Brenchley JM, Hirsch VM. 2020. Simian immunodeficiency virus-infected memory CD4+ T cells infiltrate to the site of infected macrophages in the neuroparenchyma of a chronic macaque model of neurological complications of AIDS. mBio 11:e00602-20. https://doi.org/10.1128/mBio.00602-20.

Invited Editor Robert F. Siliciano, Johns Hopkins University School of Medicine

Editor Diane E. Griffin, Johns Hopkins Bloomberg School of Public Health

Address correspondence to Vanessa M. Hirsch, vhirsch@niaid.nih.gov.

Received 13 March 2020
Accepted 23 March 2020
Published 21 April 2020

SIV-infected rhesus macaques with and without encephalitis, we show that immune cells invade the neuroparenchyma and increase in number in the CNS in animals with SIV-induced encephalitis (SIVE). Of these cells, both brain macrophages and brain memory CD4$^+$ T cells harbor replication-competent SIV DNA; however, only brain CD4$^+$ T cells harbored SIV DNA in animals without SIVE. These findings support use of CL757 as an important model to investigate disease progression in the CNS and as a model to study virus reservoirs in the CNS.

KEYWORDS AIDS, CD4 T cells, central nervous system infections, encephalitis, inflammation, macrophages, neuroAIDS, neuroimmunology, neurovirulence, rhesus macaque, simian immunodeficiency virus

Human immunodeficiency virus (HIV) infects cells of the immune system, such as CD4$^+$ T cells and macrophages (MΦs). HIV can enter the central nervous system (CNS) early in the course of infection (1, 2), and viral replication in brain macrophages (Br-MΦs) can lead to HIV-associated neurocognitive disorders (HAND) in 20 to 30% of infected individuals in the later stages of HIV infection (3). Clinical determination of HAND is associated with the presence of multinucleated giant cells (MNGCs) at the time of autopsy due to productive infection of Br-MΦs and microglial cells, a hallmark of HIV-induced encephalitis (HIVE) (4–14). Administration of combination antiretroviral therapy (cART) can greatly reduce the incidence of fulminant HIV encephalopathy and improve cognitive function; however, a milder form of HAND, minor cognitive motor disorder (MCMD), has become more commonplace and is associated with persistence of virus in the CNS and a worse prognosis than that in fully suppressed patients (6, 15, 16).

While studies of HIV-infected patients with neurological complications of AIDS (neuroAIDS) are no longer feasible due to the efficacy of antiviral drug treatment, an examination of the older literature on the pathology of HIVE/neuroAIDS revealed that lymphocytes were frequently observed in the brains of these patients (5, 8–14). Studies of HIV-infected dementia patients are complicated by the fact that this clinical syndrome encompasses both the direct effects of virus replication in the CNS, as in HIV encephalitis, as well as opportunistic infections of the brain (cytomegalovirus [CMV], polyomavirus, and *Cryptococcus* spp., to name a few) and lymphoma. In a majority of cases, opportunistic infections in the brain were identified, in addition to microglial nodules, MNGCs, and lymphoproliferative lesions of the neuroparenchyma (8, 13). Progressive diffuse leukoencephalopathy (PDL) and multifocal giant cell encephalitis (MGCE) was observed in most cases examined. MGCE was characterized by perivascular and parenchymal infiltrates of both macrophages and lymphocytes (5, 13). In these patients, a spectrum of neurological abnormalities existed, along with varied expression of neurological symptoms. Severe dementia was observed in patients with perivascular and parenchymal macrophages, as well as MNGCs, while milder cases of dementia were noted in the patients with scattered perivascular lymphocytes and macrophages (5). The authors also noted that even in severe cases of dementia, histopathological findings were nonexistent, leading them to note that histopathology is not uniform in cases of HIV-induced dementia. The pathophysiology differs from patient to patient; thus, it becomes important to have various animal models that can cover all complexities of the disease.

Simian immunodeficiency virus (SIV)-infected nonhuman primates are widely used as a model for AIDS pathogenesis. Infection of these animals with neurotropic SIV can result in SIV-induced encephalitis (SIVE)/neuroAIDS), with neuropathologic findings reminiscent of HIVE in humans, including the presence of MNGCs. SIV infection of rhesus macaques (RMs) allows for sampling of the cerebrospinal fluid (CSF) and brain tissue throughout all stages of disease progression under controlled conditions. Current models that dominate studies evaluating SIVE include the use of immunomodulation in order to induce rapid progression to neuroAIDS. One model uses pigtailed macaques coinoculated with a neurovirulent clone virus, SIVmac17E-Fr (17E-Fr), and an immuno-

TABLE 1 Animals used in study

Animal ID	Virus	Symbols and color used	Plasma viral load (vRNA[a] copies/mL)	CSF viral load (vRNA copies/mL)	W.P.I.[b] euthanized	SIVE[c] infection status
CL86	SIVMac239	✱	$1.9x10^6$	$2.7x10^4$	43	non-SIVE
H848	SIVsmmE660	▲	$1.1x10^6$	$3.1x10^3$	72	non-SIVE
H806	SIVsmmE660	▲	$3.4x10^6$	$5.5x10^3$	260	non-SIVE
H872	SIVsmmE660-SS	■	$1.3x10^6$	$1.7x10^3$	101	non-SIVE
H879	SIVsmmE660-SS	■	$1.2x10^6$	$2.3x10^3$	105	non-SIVE
H870	SIVsmmE660-SS	■	$6.2x10^5$	$2.9x10^4$	125	non-SIVE
H834	SIVsmmE543-3-SS	▼	$4.5x10^5$	$6.8x10^2$	174	non-SIVE
H891	SIVsmmE543-CT	★	$1.2x10^6$	$5.5x10^3$	65	non-SIVE
H892	SIVsmmE543-CT	★	$7.4x10^6$	$2.7x10^4$	56	non-SIVE
H883	SIVsmm804E-CL757	●	$3.0x10^5$	7.6×10^3	98	non-SIVE
H884	SIVsmm804E-CL757	●	$1.6x10^6$	$4.6x10^4$	105	non-SIVE
H886	SIVsmm804E-CL757	●	$3.2x10^6$	$4.6x10^6$	54	SIVE
H882	SIVsmm804E-CL757	●	$2.4x10^6$	$1.4x10^7$	68	SIVE
H887	SIVsmm804E-CL757	●	$2.4x10^6$	$1.6x10^8$	54	SIVE

[a]vRNA, viral RNA.
[b]W.P.I., weeks postinfection.
[c]SIVE, SIV-induced encephalitis.

suppressive, uncloned virus, SIVsmB670 (17). This dual infection model results in the peripheral depletion of $CD4^+$ T cells by B670, which appears to allow for efficient replication of 17E-Fr in Br-MΦs. The advantage of this model is high reproducibility of SIVE in animals (90%); however, animals rapidly progress to neuroAIDS within 3 to 6 months postinfection. A second model uses immunomodulation to induce neuroAIDS. RMs are administered anti-CD8 antibodies prior to inoculation with SIV (SIVmac251 or SIVmac239), and just as with the pigtailed macaques, animals rapidly progress within 3 to 6 months postinfection (18, 19). A third model uses anti-CD4 antibodies to deplete $CD4^+$ T cells in RMs prior to infection with SIVmac251. This results in a rapid progression to neuroAIDS within 3 months postinfection due to productive infection in microglia (20, 21).

We have recently reported on this SIVE/neuroAIDS model using uncloned SIV isolated after 4 serial passages of nonneurovirulent SIVsmE543-3 (E543-3) through RMs and subsequently generated a neurovirulent molecular clone virus, SIVsmm804E-CL757 (CL757) (22). Infection with this clone virus leads to SIVE in 50% of infected RMs approximately 1 year postinfection. In the current study, we examined the brains of RMs infected with CL757 and other nonneurovirulent strains of SIV from sooty mangabey monkeys (SIVsmm) to identify which cellular subsets in the brain are targeted by the virus. We show that in macaques that conventionally progress to neuroAIDS, both brain memory $CD4^+$ cells (Br-mCD4s) and Br-MΦs harbor replication-competent SIV DNA. We also show that Br-mCD4s harboring SIV DNA infiltrate the neuroparenchyma and localize to the site of viral replication. Unexpectedly, Br-mCD4s harbored SIV DNA in animals that showed no pathological or clinical signs of neuroAIDS. This finding indicates an unanticipated role for Br-mCD4s as a potential additional viral reservoir.

RESULTS

Mononuclear cells increase in numbers in the CNS of conventional progressor macaques with SIVE. We analyzed the immune cell populations isolated from saline-perfused, whole-brain tissue of SIV-infected RMs harvested ($n = 14$) at disease end points (Table 1). The animals used in this study were taken from a variety of different studies as they became available. This included a subset of the animals inoculated with

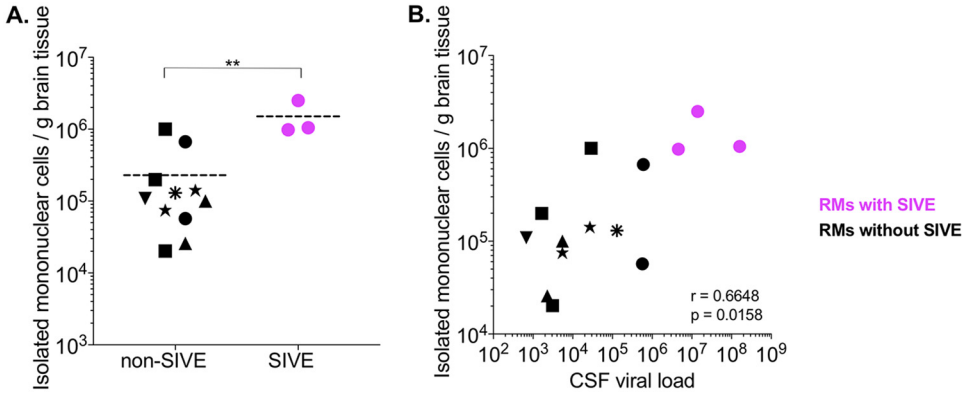

FIG 1 Mononuclear cell population increases in the brains of RMs with SIVE. Mononuclear cells were isolated from homogenized brain tissue taken from RMs with and without SIVE ($n = 14$). Cells were counted and normalized to grams of brain tissue homogenized. Each symbol represents groupings of animals infected with a different virus strain. Pink symbols represent rhesus macaques that were confirmed to have SIV-induced encephalitis, and black symbols represent nonencephalitic macaques. (A) Average number of mononuclear cells per gram of brain tissue in RMs without SIVE compared to RMs with SIVE ($P = 0.0088$). Groups were compared by nonparametric Mann-Whitney test. The dotted line represents the median value. (B) Correlation of mononuclear cells per gram of brain tissue and the viral load within the CSF ($n = 14$). Statistics were calculated using the Spearman correlation.

the neurotropic clone CL757, described previously (22). In a study by Matsuda et al. (22), 8 animals were inoculated with CL757, and only 4 animals developed neuroAIDS. For our current study, we were only able to use 3 of the 4 animals that developed SIVE (H882, H886, and H887) to isolate mononuclear cells, as one animal (H880) exhibited acute neurologic signs that necessitated prompt euthanasia, so proper tissue collection was not feasible. The remaining animals examined in this current study were inoculated with related SIVsmm virus strains ($n = 8$), CL757 ($n = 2$), or SIVmac239 ($n = 1$) and served as SIV-infected controls without SIVE. Whole-brain tissue was removed for histopathologic and cellular analysis. Half of the brain tissue from each animal was paraffin embedded and the other half mechanically and enzymatically homogenized. Homogenized brain tissue included cells of the parenchyma, choroid plexus, and meningeal layers. Homogenized tissue was then separated over a discontinuous Percoll gradient, and mononuclear cells were harvested at the interface. Isolated mononuclear cells were first counted and then stored in liquid nitrogen in a freezing medium of 90% fetal bovine serum with 10% dimethyl sulfoxide (DMSO).

We first observed an increase in the number of mononuclear cells recovered from the brains of animals with SIVE compared to that found in the other study animals (Fig. 1). The concentration of mononuclear cells from RMs without SIVE averaged 1.1×10^5 cells/gram of brain tissue ($n = 11$), whereas the concentration of cells isolated from RMs with SIVE averaged 1.1×10^6 cells/gram of brain tissue ($n = 3$), a significant increase ($P = 0.011$) in mononuclear cells over that in non-SIVE animals (Fig. 1A). This increase correlated with an increase in the CSF viral load ($r = 0.6648$, $P = 0.0158$) (Fig. 1B). We next employed live-cell sorting to characterize the cellular subsets of isolated brain mononuclear cells. We gated on live cells and measured subsets expressing CD3, CD4, CD20, CD11b, HLA-DR, CD28, and CD95 as a percentage of $CD45^+$ cells (Fig. 2A). Analysis showed significant increases in the percentage of Br-CD4s (Fig. 2B), Br-MΦs (Fig. 2C), and brain B cells (Br-B cells) (Fig. 2D) isolated from the brains of RMs with SIVE. Br-CD4s consisted mainly of memory $CD4^+$ T cells (mCD4s) that increase in the brains of RMs with SIVE (Fig. 2E). These data suggest that an increase in the number of CD4, MΦs and B cells occur in the brain compartment in RMs with SIVE that have progressed to neuroAIDS at a conventional pace, consistent with an inflammatory process.

Br-mCD4s harbor replication-competent virus. We isolated Br-mCD4s and Br-MΦs from mononuclear cells by flow cytometric sorting to determine if these cells harbored SIV DNA. From the brain mononuclear cells, 3×10^5 Br-mCD4s and Br-MΦs

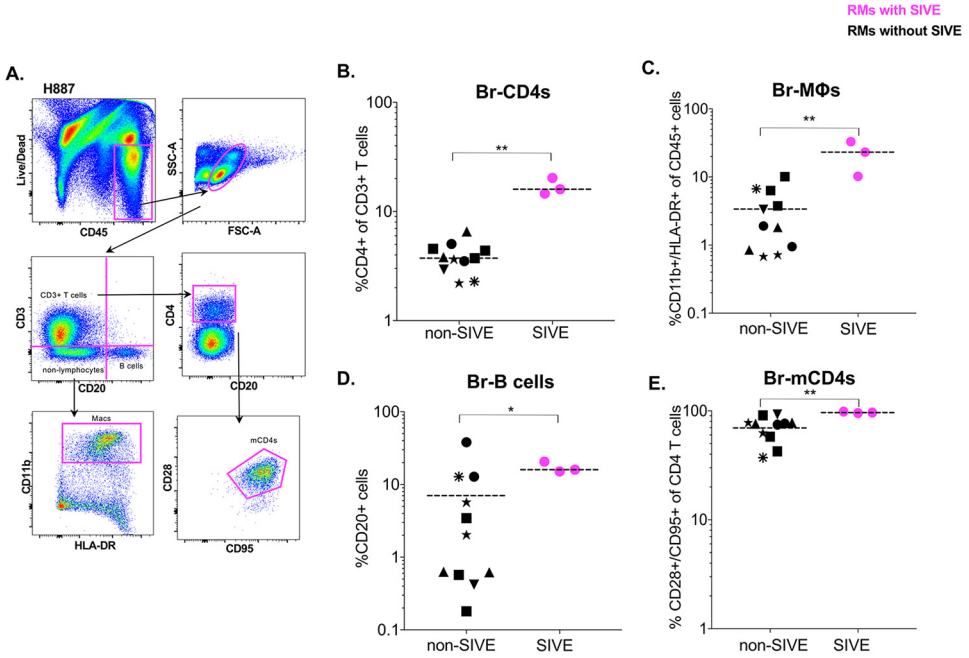

FIG 2 Cellular subsets of brain mononuclear cells in rhesus macaques with and without SIVE. Mononuclear cells isolated from RM brain tissue were stained with monoclonal antibodies to identify the relative proportions of T cell subsets and macrophages. (A) The gating strategy for sorting of mCD4s and macrophages is as follows: top, live versus CD45 to identify the leukocyte population, and then side scatter area (SSC-A) versus forward scatter area (FSC-A) gated on lymphocytes and monocytes; middle, CD3 versus CD20 to isolate $CD3^+$ lymphocytes and identify/exclude B cells from the remaining nonlymphocyte population. CD3 cells versus CD4 and the $CD4^+$ populations were stained with CD28 and CD95 to identify memory ($CD28^+$ $CD95^+$) subsets. Bottom, CD11b versus HLA-DR of the nonlymphocyte ($CD3^-$ $CD20^-$) population to identify and isolate macrophages ($CD11b^+$ $HLA\text{-}DR^+$). (B to D) $CD4^+$ T cells ($P = 0.0055$) (B), macrophages ($P = 0.0055$) (C), and B cell populations ($P = 0.0357$) (D) showed significant increases in RMs with SIVE. (E) Br-CD4s are mainly a memory phenotype and increase in the brains of RMs with SIVE ($P = 0.0055$).

were sorted, along with the same number of peripheral blood mCD4s (P-mCD4s), and assessed for SIV DNA by quantitative PCR (Fig. 3A). Br-mCD4s isolated from each animal harbored copies of SIV DNA, as did P-mCD4s, while Br-MΦs containing viral DNA were only found in RMs with SIVE (H882, H886, and H887; Fig. 3A).

Macrophages are known to phagocytose pathogens and dying cells, and it has been previously shown that tissue myeloid cells acquire viral DNA via phagocytosis of SIV-infected $CD4^+$T cells. We therefore measured levels of rearranged T-cell receptor (TCR) DNA in both Br-mCD4s and Br-MΦs of RMs with SIVE (H886, H887, and H882). The levels of rearranged TCR DNA were low compared to what has been observed in macrophages in other tissues (23). Between 0.1 and 6.5% of brain macrophages had detectable rearranged TCR DNA (data not shown). These levels are insufficient to account for the levels of viral DNA we see in Br-MΦs, negating the premise that the viral DNA in these myeloid cells could be attributed to CD4 T cell phagocytosis, even though there were CD4 T cells infiltrating the brain.

To evaluate whether the viral DNA observed in the brain was replication competent, additional sorted cells from the peripheral blood and brain of CL757-infected RMs with SIVE (H882 and H887) and without SIVE (H883 and H884) were cocultured with CEMx174 cells. These cells are highly susceptible to SIV infection and support viral replication better than do monocyte-derived macrophages or primary $CD4^+$ T cells. Br-mCD4s, Br-MΦs, and P-mCD4s from RMs with SIVE, H882, and H887 (8×10^3) were mixed with 4×10^5 CEMx174 cells, and the supernatants were harvested every 3 to 4 days for 2 weeks and checked for virus presence by reverse transcriptase activity. We were unable to analyze cells from H886 by coculture since the cells were not viable. The virus isolation results paralleled those from the quantitative PCR (qPCR). Thus, virus was

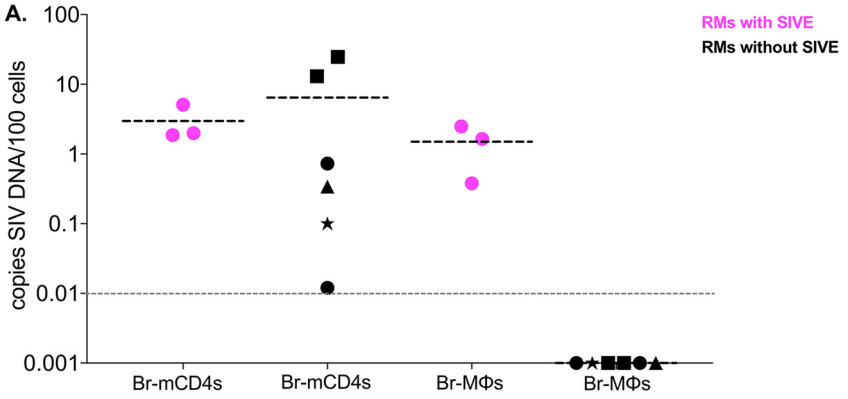

B.

Animal ID	SIVE	Virus Isolation/qPCR: Brain mCD4s	Brain MΦs	PBMCs mCD4s
H882	+	+/+	+/+	+/+
H886	+	ND/+	ND/+	ND/+
H887	+	+/+	+/+	+/+
H883	-	-/-	-/-	+/+
H884	-	-/-	-/-	+/+

Abbreviations: a. ND, not done

FIG 3 Brain mCD4s from SIV-infected RMs harbor SIV DNA. (A) Total SIV-DNA measured by standard *gag* reverse transcriptase (RT-PCR) ($n = 9$). Dotted lines represent the median value. (B) RMs infected with molecular clone CL757 are cocultured with CEMx174 cells. Viral activity was measured by RT activity. +, samples in which both RT activity was detected and qPCR was positive; ND, not done.

isolated from mCD4s of blood mononuclear cells (PBMCs) and the brains of all animals, but only Br-MΦs isolated from RMs with SIVE yielded infectious virus (Fig. 3B). These results show that only macrophages isolated from macaques with SIVE harbored infectious SIV. In contrast, infectious virus was present in Br-mCD4s of all of the SIV-infected animals assessed, regardless of whether they exhibited SIVE.

Lymphocyte-rich regions in the neuroparenchyma of conventional progressor macaques. Conventional progressor (CP) RMs with SIVE H882, H886, and H887 exhibited increased mononuclear cell counts in the brain homogenates due to an increase in mCD4s, MΦs, and B cells (Fig. 2). In our previous study, lesions encompassing lymphocytes were observed by immunohistochemistry (IHC) in the neuroparenchyma of CP RMs with SIVE (24). These lymphocyte-rich lesions have not been previously reported before in RP RMs suffering from SIVE. We performed additional IHC on paraffin-embedded brain sections from both CP (H886) and historical sample (H583) RP RMs. We chose a panel of monoclonal antibodies to identify myeloid cells and lymphocytes similar to those used for our flow analysis, as follows: anti-CD3, anti-CD4, which also labels macrophages, anti-CD8, anti-CD20 (B cells), and a dual staining with anti-CD68 and anti-CD163 for myeloid cells. Both H886 and H538 exhibit previously observed pathological signs of SIVE, which includes perivascular accumulation (cuffing) of MΦs and MNGCs (Fig. 4A). MNGCs were surrounded by $CD3^+$ cells (Fig. 4B), which mainly consisted of $CD4^+$ cells (Fig. 4C) and $CD8^+$ cells (Fig. 4D), with some B cells ($CD20^+$; Fig. 4E) in the parenchyma. This result suggests that inflammatory cells infiltrate the neuroparenchyma of CP macaques and localize to the site of viral replication.

Lymphocyte-rich lesions in the neuroparenchyma are the site of viral replication. Previous studies have shown that MΦs are the chief target cell in the brain for HIV/SIV replication in association with encephalitis. Our studies support that finding since SIV-infected MΦs were only observed in the brain of macaques with SIVE. We hypothesized that mCD4s infiltrate the brain from the periphery in response to viral replication in MΦs and harbor viral DNA, thus potentially serving as a cellular reservoir

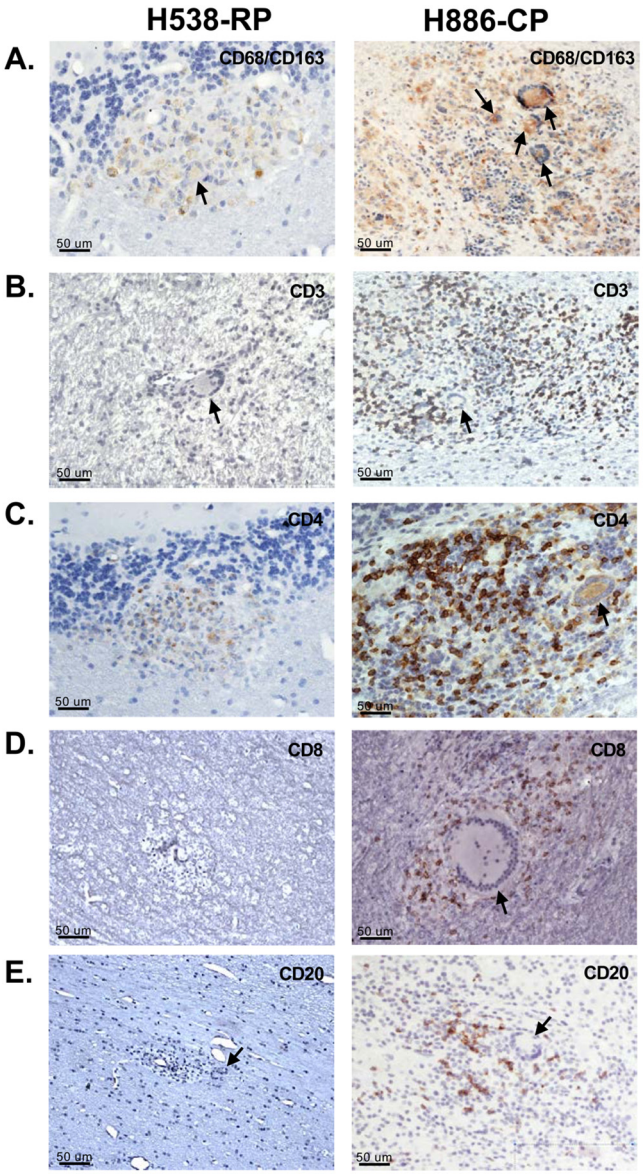

FIG 4 Infiltration of lymphocytes into the neuroparenchyma of SIVE conventional progressor macaques. Shown are immunohistochemistry images representing confirmed SIVE RMs, one with rapid progressor (RP) to SIVE (H538) and one with conventional progressor (CP) to SIVE (H886). (A to E) Slides were stained with CD68/CD163 to identify myeloid/macrophages (A), CD3 to identify lymphocytes (B), CD4 to identify $CD4^+$ T cells (C), CD8 to identify $CD8^+$ T cells (D), and CD20 to identify B cells (E). All sections were then stained with DAB substrate (brown) and counterstained with hematoxylin (blue). Black arrows point to multinucleated giant cells.

for virus in the brain. Using immunofluorescence in conjunction with DNAscope, we immunophenotyped cells to visualize the location of $CD4^+$ T cells harboring SIV DNA in the brain. Using paraffin-embedded brain sections and the same panel of antibodies from the aforementioned IHC experiment, we identified $CD4^+$ T cells (green), $CD68^+$/$CD163^+$ myeloid lineage cells (blue), and SIV DNA (red) using sense probes that target the 5′ *gag-pol* portion of the SIVmac239 genome located in the nucleus (cyan) (Fig. 5). Examination of midbrain sections of an RM with SIVE, H886, identified multiple lymphocyte-rich lesions located throughout the neuroparenchyma (Fig. 5A). Upon closer inspection, we discovered that infiltrating Br-mCD4s, as well as Br-MΦs, overlapped the SIV DNA signal (Fig. 5B). We also performed RNAscope on these same sections using anti-sense probes that target viral genes in the 3′ section of the SIV

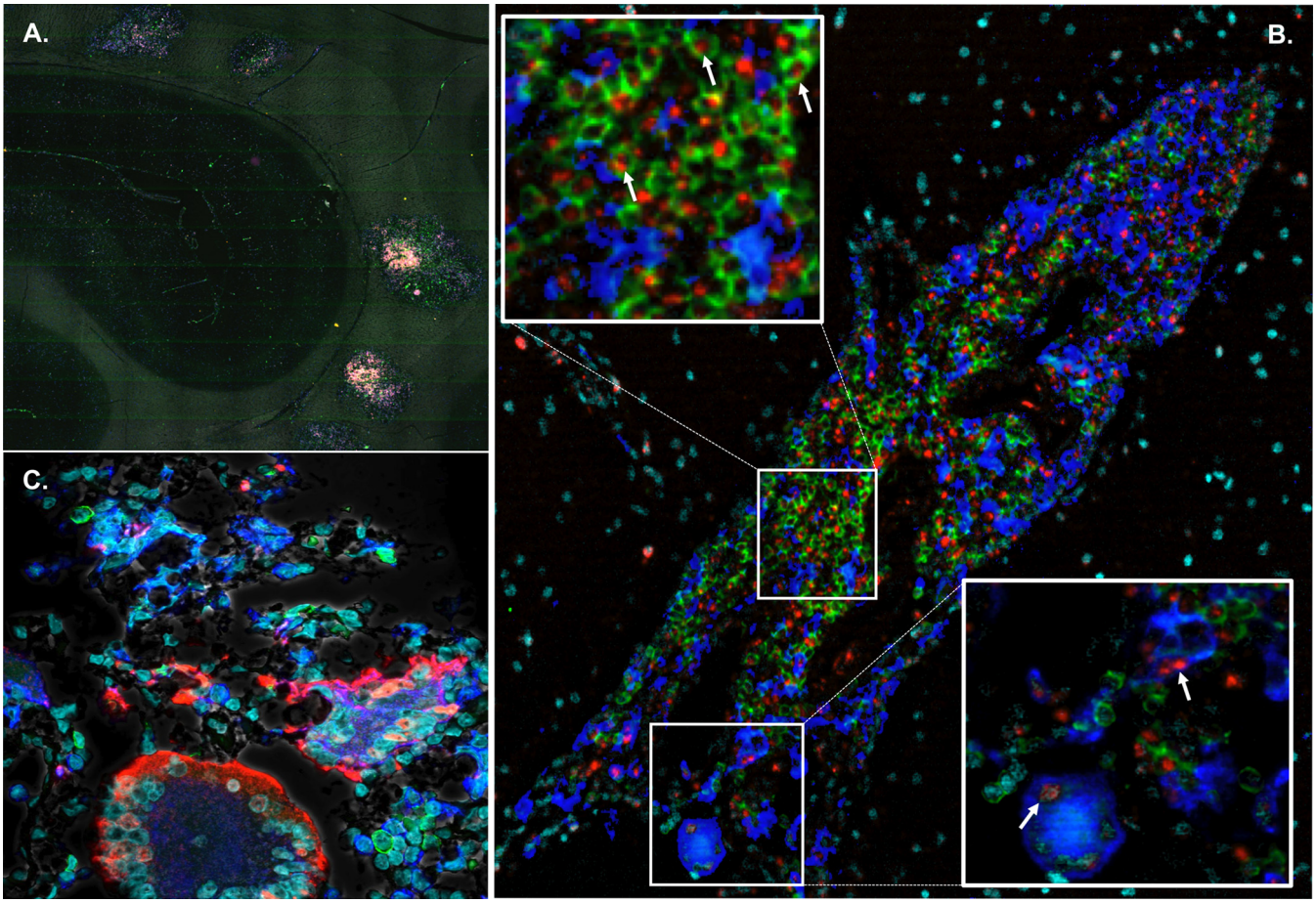

FIG 5 DNAscope and RNAscope of lymphocyte-rich lesions in the neuroparenchyma of RMs with SIVE. SIV DNAscope and RNAscope were combined with immunofluorescence. Shown are representative images of the brain with SIV DNA (red), with staining for CD4 (green) to identify T cells, a combination of CD163 and CD68 markers (blue) to identify myeloid/macrophage cells, and DAPI (cyan) to identify the nucleus. (A) Tiled image of a brain section from H886 showing multiple lesions located at various positions in the neuroparenchyma/white matter of the midbrain. (B) A ×20 image of the meninges in H887 showing an accumulation of CD4 T cells and myeloid/macrophages harboring SIV DNA. The top inset image shows a close-up of SIV-infected $CD4^+$ T cells, and the bottom inset image shows in detail a multinucleated giant cell with surrounding macrophages and $CD4^+$ T cells positive for SIV DNA in the nucleus. White arrows point to the nucleus harboring SIV DNA. (C) RNAscope showing multinucleated giant cells are sites of actively replicating virus. SIV RNA is labeled in red.

mac239 genome (*vif*, *vpx*, *vpr*, *tat*, *env*, and *nef*) to determine whether cells with viral DNA in these lesions are transcriptionally active (Fig. 5C). These data show that MGNCs are indeed a site of active viral replication and that Br-mCD4s harboring SIV DNA localize to the site of viral replication in the neuroparenchyma. We also performed DNAscope on paraffin-embedded brain sections from RMs without SIVE (H883 and H884). Despite the identification of viral DNA in Br-CD4s by qPCR and infectious virus by coculture, we were not able to able to identify SIV DNA^+ Br-CD4s in the CNS of either RM without encephalitis. Presumably, this is due to the low numbers of CD4s infiltrating the CNS in the absence of encephalitis (data not shown), as indicated by the low recovery of mononuclear cells from these animals (Fig. 1).

DISCUSSION

Shortly after infection, HIV establishes itself in the CNS where it persists throughout the course of disease and in untreated patients eventually results in encephalitis and neuroAIDS. Although the mechanism of entry into the CNS remains unknown, a hallmark of HIVE/neuroAIDS is the infection and replication of HIV in macrophages and the resulting formation of multinucleated giant cells (MNGCs). Studies of neuroAIDS in HIV-infected individuals are difficult due to the limitations of direct sampling of the CNS; therefore, animal models that closely resemble the disease conditions in humans

are of utmost importance. We used one such model of neuroAIDS that results in a conventional (rather than rapid) disease progression and results in SIVE/neuroAIDS in about half of the inoculated macaques to study the cellular targets in the brain at terminal disease endpoints. Using isolated CNS mononuclear cells and tissue from a panel of chronically infected RMs, we demonstrate that the development of SIVE in CP RMs leads to the formation of lymphoid-rich lesions that are associated with glial nodules and MNGCs at the site of chronic viral replication and inflammation in the neuroparenchyma. In RMs without SIVE, viral DNA was not found in Br-MΦs; however, replication-competent viral DNA was discovered in the Br-mCD4s. The finding of virus in the Br-mCD4s of RMs with or without SIVE was unexpected since most studies have focused on the role of MΦs in this disease process. Indeed, MΦs appear to be the sole cell type harboring SIV in the brains of RP RMs with SIVE and are clearly strongly associated with the pathology of SIVE. Infection of macrophages was only observed in association with pathological evidence of encephalitis linking this cell type to the pathogenesis of inflammation in the CNS in neuroAIDS. Our current model can aid in the elucidation of the pathophysiology of neuroAIDS using CP RMs and indicates an unanticipated role for mCD4s as an additional potential viral reservoir in the CNS.

Recruitment of T cells to the CNS has been previously reported in cases of CNS disease, although these studies have focused predominately on brain $CD8^+$ T cells isolated from RMs that rapidly progressed to SIVE (25, 26). Lymphocyte infiltration of the CNS is thought to arise due to hematopoietic lymphocytes surveying the CNS via the meninges and choroid plexus and encountering their cognate antigen presented by an antigen-presenting cell (APC)/Br-MΦs, which leads to two subsequent events. First, cells are trafficked in through high-endothelial vessels and localize to the site of virus infection (27, 28); second, mCD4s clonally expand in attempt to control and clear infection (29, 30). Past examinations of HIV-infected patients with neuroAIDS, prior to the discovery of antiretroviral drug treatment, showed that along with the development of MNGCs, lymphocytes were present in the neuroparenchyma of these patients (5, 8–14). These past studies show that histopathology is not uniform in cases of AIDS-induced dementia. The pathophysiology of brain sections differed from patient to patient, even in those with severe cases of dementia; thus, it becomes important to have various animal models that can cover all complexities of the disease.

We examined tissue and mononuclear cells isolated from the CNS from a panel of 15 RMs all chronically infected with either CL757 ($n = 5$) or other relevant SIVsmm strains ($n = 10$). Three CL757-infected RMs developed SIVE, as determined by high CSF viral loads (VLs) and MNGCs, which are indicators of viral replication in Br-MΦs. Inflammatory responses initiated from infected MΦs have been previously shown to recruit adaptive immune cells from the periphery to the target tissue, with these infiltrating cells consisting mainly of T cells, B cells, and MΦs (31, 32). We observed a significant increase in the number of mononuclear cells in the brains of animals with SIVE and identified classical adaptive immune cells, $CD4^+$ and $CD8^+$ T cells, B cells, and MΦs, within this population. There were significant increases in the percentages of $CD4^+$ T cells, B cells, and MΦs, all of which correlated with an increase in the CSF viral load, while the population of $CD8^+$ T cells remained constant regardless of the SIVE status of the animal. Of the $CD4^+$ and $CD8^+$ T cells isolated from the CNS, they were all of a memory phenotype, which confirmed previously reported findings that lymphocytes of the CNS are mainly of the memory subset (33). Br-MΦ populations have previously been shown to expand proportionally with the formation of MNGCs due to the proliferation of infected MΦs (34). Using an immunofluorescence assay (IFA) coupled with both DNA and RNAscope, we see that RMs with SIVE harbor SIV DNA that is transcriptionally active in Br-MΦs within lymphoid-rich lesions. We have previously shown that CL757 is highly adapted to replicate in the CNS compared to its parental clone, SIVsmmE543-3 (E543-3), which is generally excluded from replicating in the CNS (22). Our study shows that while trafficking does occur between the CNS and the periphery, Br-mCD4s appear to harbor replication-competent virus in the CNS in the absence of SIVE. This consistent with CD4s trafficking from the periphery to the CNS,

which may allow for the CNS to serve as a reservoir for SIV in Br-mCD4s. Since this study did not examine target cells in the brain during primary infection or following the initiation of antiretroviral therapy (ART), we can only speculate as to the initial targets for virus in the CNS and the persistent reservoir. Further studies will be required to determine whether mCD4s constitute a significant reservoir in fully cART-suppressed macaques with critical implications for eliminating the viral reservoir to effect a cure.

In summary, variations in neurological disease outcomes are common in HIV-infected individuals. Studies of neuroAIDS in humans are complicated by limitations on samples collected and the widespread use of antiviral drug therapy, which has greatly reduced the incidence of fulminant HIVE/neuroAIDS. CL757-infection of RMs leads to the development of SIVE/neuroAIDS at a conventional pace closely resembling the tempo of disease in HIV-infected patients. This model shows infiltration and/or proliferation of classical adaptive immune cells to the CNS of RMs with SIVE, and of these, a high percentage are MΦs and mCD4s. Both cell types are carriers of replication-competent SIV DNA and, along with B cells, localize to the site of viral replication in the neuroparenchyma. While SIV-infected RMs without SIVE do not harbor virus in Br-MΦs, mCD4s harbored replication-competent SIV DNA in such animals, implicating mCD4s as a potential long-term viral reservoir in the brain.

MATERIALS AND METHODS

Ethics statement and animal studies. This study was carried out in strict accordance with the recommendations described in the Guide for the Care and Use of Laboratory Animals of the National Institutes of Health, the Office of Animal Welfare, and the U.S. Department of Agriculture. Colony-bred rhesus macaques of Indian origin were obtained from the Morgan Island, SC, rhesus monkey breeding colony. All animal work was approved by the NIAID Division of Intramural Research Animal Care and Use Committee (IACUC) in Bethesda, MD (animal study protocol LMM-6). The animal facility is accredited by the American Association for Accreditation of Laboratory Animal Care. All procedures were carried out under ketamine anesthesia by trained personnel under the supervision of veterinary staff, and all efforts were made to ameliorate the welfare of the animals and to minimize animal suffering in accordance with the recommendations of the Weatherall report on the use of nonhuman primates. Animals were housed in adjoining individual primate cages, allowing for social interaction, under controlled conditions of humidity, temperature, and light (12-h light/12-h dark cycles). Food and water were available *ad libitum*. Animals were monitored twice daily (pre- and postchallenge) and fed commercial monkey chow, treats, and fruit twice daily by trained personnel. Early endpoint criteria, as specified by the IACUC-approved score parameters, were used to determine when animals should be humanely euthanized.

Study animals and sample processing. This study consisted of 14 chronically infected SIV-infected RMs (3 RMs chronically infected with variants of SIVsmmE543-3, 5 RMs with variants of SIVsmmE660, 1 RM with SIVmac239, and 5 RMs with SIVsmm804E-CL757; Table 1). Viral clones designated with "SS" were distinguished by the introduction of a double mutation, P37S-R89S, in the Gag protein that conferred resistance to TRIM-5^{TFP} restriction, and viral clones designated with "CT" encoded an Env protein in which the entire cytoplasmic was truncated (35–38). Although all study animals were evaluated at terminal disease endpoints, neuroAIDS was only observed in those animals inoculated with CL757. Peripheral blood was collected from all animals terminally, and peripheral blood mononuclear cells (PBMCs) were isolated via standard density gradient centrifugation using LSM solution (MP Biomedicals, Santa Ana, CA) and then analyzed from frozen samples attained at necropsy. Brain tissue from each animal was processed fresh, and mononuclear cells were isolated from frozen samples and analyzed.

Isolation of brain mononuclear cells. All animals were saline perfused before necropsy to remove blood from the tissues. Whole brain was sliced in half along the sagittal plane, and one half was preserved in neutral-buffered 10% formalin solution (Sigma-Aldrich) for subsequent histopathology immunohistochemistry and DNAscope/RNAscope. The remaining half of the brain was used to isolate mononuclear cells using a protocol adapted from a study by Cardona et al. (39). Briefly, tissue was diced and then enzymatically digested for 1 h in digestion solution composed of Hanks' balanced salt solution (HBSS) without Ca^{2+} and Mg^{2+} (Sigma-Aldrich), supplemented with 0.05% collagenase D (catalog no. 110-888-82-001; Sigma), 0.5% Dispase II (catalog no. D4693-1G; Sigma), 0.025 U/ml DNase I (catalog no. D4527-10KU; Sigma), and 0.025 U/ml *Nα-p*-tosyl-L-lysine chloromethyl ketone [TLCK] (catalog no. T7254-100 mg; Sigma) at 37°C with agitation (39). Homogenized tissue was centrifuged at 300 × *g* for 10 min and the cell pellet washed with 1× HBSS twice to remove any residual enzymes. The washed pellet was resuspended at a 1:1 ratio in 100% Percoll (diluted with 1× HBSS). A Percoll gradient was formed using 10 ml of 70% Percoll and 1× HBSS in the bottom of a 50-ml conical tube and then overlaid with 15 ml homogenized tissue mixed with equal parts of undiluted Percoll solution. Ten milliliters of 30% Percoll solution was slowly layered on top, followed by 15 ml of 1× HBSS, and the gradient was centrifuged for 40 min at 500 × *g*. Cells were harvested from the 30 to 50% interphase and washed with 1× HBSS 3 times to remove residual Percoll, and the cells were suspended in 10 ml of 1× HBSS. Cells were cryopreserved in freezing medium (90% fetal bovine serum and 10% DMSO) in liquid nitrogen.

Immunophenotyping. Polychromatic cell sorting was performed on stained mononuclear cells isolated from fresh rhesus macaque brain tissue utilizing a FACSAria II flow cytometer (BD Biosciences, Franklin Lakes, NJ) equipped with the FACSDiva software (BD Biosciences). Cells were first stained with a LIVE/DEAD fixable aqua dead cell dye (Life Technologies, Carlsbad, CA). For live-cell sorting, the following panel of monoclonal antibodies (MAbs) was used: CD14 fluorescein isothiocyanate (FITC; clone M5E2), BD CD123 phycoerythrin (PE; clone 6H6; Pharmingen), CD28 ECD (clone CD28.2; BioLegend), CD95 PECy5 (clone DX2; Beckman Coulter), CD11c BV605 (clone 3.9; BioLegend), HLA-DR APC-H7 (clone L243; BioLegend), CD4 BV650 (clone OKT4; BD), CD11b BV785 (clone ICRF44; BioLegend), CD45 V450 (clone D058-1283; BioLegend), CD206 APC (clone 19.2; BD Horizon), CD3 Alexa700 (clone SP34-2; BD Pharmingen), and CD20 PE-Cy7 (clone L27; BD Pharmingen). The results were analyzed using the FlowJo software v9.9 (TreeStar, Ashland, OR). A threshold cutoff of 200 cells of the parent population was used for all cell subset analyses.

Quantitative PCR for SIV DNA. From isolated brain mononuclear cells, we sorted 30,000 live memory $CD4^+$ T cells (live, $CD45^+$ $CD3^+$ $CD4^+$ $CD28^+$ $CD95^+$) and 30,000 live MΦs (live, $CD45^+$ $CD4^+$ $CD20^-$ $CD11b^+$ $HLA\text{-}DR^+$) cell populations using a BD FACSAria II flow cytometer and then lysed the sorted cells with 25 μl of a 1:100 dilution of proteinase K (Roche, Indianapolis, IN) in 10 mM Tris buffer. We performed quantitative PCR with 5 μl of cell lysates per reaction using the following reaction conditions: 95°C for 5 min and 40 cycles of 95°C for 15 s, followed by 60°C for 1 min. We used TaqMan gene expression master mix (Life Technologies) with the following primers and probes against SIVsmE543: For, GGC AGG AAA ATC CCT AGC AG; Rev, GCC CTT ACT GCC TTC ACT CA; and probe, AGT CCC TGT TCR GGC GCC AA. A StepOnePlus PCR machine and software (Applied Biosystems) were used to amplify genes of interest.

Immunohistochemistry for lymphocytes. Brain tissue was collected at the time of necropsy and preserved in 10% neutral-buffered formalin solution (HT501128; Sigma). Tissue sections were then embedded in paraffin and made into unstained slides cut to 5-μm thickness by American Histolabs, Inc. (Gaithersburg, MD). For CD3, CD4, CD20, and joint CD63/CD168 (for myeloid lineage cells) staining, slides were heated at 60°C for 1 h and deparaffinized in xylene washes and 50% xylene–50% ethanol wash, and then they were rinsed twice in 100% ethanol. Tissues were then slowly rehydrated with a series of ethanol and double-distilled water (ddH_2O) washes, added to boiling Target Retrieval solution (catalog no. 32200; ACDBio) for 30 min at 98°C, and then washed in 1× Tris-buffered saline with Tween 20 (TBST) buffer. For CD8 staining, tissues were deparaffinized, rehydrated, and heated in Trilogy pretreatment solution (Calle Marque, Rocklin, CA, USA), using a pressure cooker at 110 to 120°C for 15 min, and then hot washed with Trilogy solution, followed by a second hot wash with 1× TBST. All slides were then treated with 0.03% hydrogen peroxide reagent for 30 min and then incubated at room temperature for 2 h with 10% goat normal serum (Vector Laboratories, Burlingame, CA). Slides were incubated with primary antibodies overnight at 4°C with dilutions as follows: rabbit monoclonal anti-CD3, 1:200 (clone SP7; Thermo Scientific); rabbit monoclonal anti-CD4, 1:200 (clone EPR6855; Abcam); rabbit monoclonal anti-CD8, 1:50 (clone SP16; Invitrogen); mouse monoclonal anti-CD20, 1:200 (clone L26; Dako); mouse monoclonal anti-CD68, 1:400 (clone KP1; BioCare Medical); and mouse monoclonal anti-CD163, 1:400 (clone 10D6; Leica Biosystems). Secondary antibodies (1:1,000, goat anti-mouse horseradish peroxidase [HRP], ab205719; and goat anti-rabbit HRP, ab205718; Abcam) were incubated at room temperature, and hybridization signal was detected using 3,3′-diaminobenzidine tetrahydrochloride (DAB) substrate. Slides were counterstained with chloramphenicol acetyltransferase (CAT) hematoxylin and visualized and photographed with a Zeiss Axio Imager Z1 microscope.

SIV DNAscope/RNAscope with immunofluorescence. To immunophenotype the cells containing viral DNA, we combined SIV-specific DNAscope with immunofluorescence-targeting cell markers using antibodies for T cells and myeloid lineage cells as listed above. We performed DNAscope following the protocol described above using RNAscope Probe-SIVmac239-sense (catalog no. 314071; American Cell Diagnostics [ACD]), and after the last amplification step, viral DNA was developed using the Tyramide Signal Amplification (TSA) Plus Cy3.5 kit (PerkinElmer). Next, slides were directly incubated overnight at 4°C with antibodies to phenotype T cells and myeloid lineage cells, as stated above. Slides were washed and incubated with secondary antibodies donkey anti-rabbit IgG-Alexa 488 and donkey anti-mouse Alexa 647 (all from Molecular Probes/Thermo Fisher Scientific) for 1 h at room temperature. To decrease autofluorescence, the tissues were incubated with Sudan Black solution (0.1% in 80% ethanol [ENG Scientific, Inc.] plus 1× TBS) for 30 min at room temperature, washed, counterstained with 4′,6-diamidino-2-phenylindole (DAPI) (ready to use [RTU]; ACD) for 10 min, washed in TBS, and coverslipped using the ProLong Gold reagent (Invitrogen). Tiled images were collected on a Leica DMI6000 wide-field microscope equipped with a 20×/0.4 numerical aperture (NA) objective, an EL6000 light source, appropriate filter cubes, and a DFC360FX monochrome camera. The remaining images were taken with 2 by 2 binning, and mosaic tiled images were stitched automatically using the Leica Application Suite X (LAS X) software. IFA images were visualized and photographed using a Zeiss Axio imager Z1 microscope affixed with ApoTome. RNAscope was performed as described above for DNAscope except using RNAscope Probe-V-SIVmac239-vif-env-nef-tar probe (catalog no. 416131; ACD).

Statistical analysis. Statistical analyses of cell correlations and averages were performed using Prism 285 (v7.0; GraphPad Software, Inc.). The Mann-Whitney *t* test (unpaired, nonparametric) was used to determine if there were significant differences between average populations. Analyses between the size of the mononuclear cell population and the CSF VL were calculated using the Spearman correlation.

ACKNOWLEDGMENTS

We thank Richard Herbert, Heather Cronise, and Joanna Swerczek of the NIHAC for excellent animal care.

Funding was mainly provided by the Intramural Program of the National Institute of Allergy and Infectious Diseases. This project has also been funded in part with federal funds from the National Cancer Institute, National Institutes of Health, under contract HHSN261200800001E.

The content of this publication does not necessarily reflect the views or policies of the Department of Health and Human Services, nor does the mention of trade names, commercial products, or organizations imply endorsement by the U.S. Government.

REFERENCES

1. Davis LE, Hjelle BL, Miller VE, Palmer DL, Llewellyn AL, Merlin TL, Young SA, Mills RG, Wachsman W, Wiley CA. 1992. Early viral brain invasion in iatrogenic human immunodeficiency virus infection. Neurology 42:1736–1739. https://doi.org/10.1212/WNL.42.9.1736.
2. Milush JM, Chen HL, Atteberry G, Sodora DL. 2013. Early detection of simian immunodeficiency virus in the central nervous system following oral administration to rhesus macaques. Front Immunol 4:236.
3. Navia BA, Jordan BD, Price RW. 1986. The AIDS dementia complex: I. Clinical features. Ann Neurol 19:517–524. https://doi.org/10.1002/ana.410190602.
4. Sharer LR, Cho ES, Epstein LG. 1985. Multinucleated giant cells and HTLV-III in AIDS encephalopathy. Hum Pathol 16:760. https://doi.org/10.1016/S0046-8177(85)80245-8.
5. Navia BA, Cho E-S, Petito CK, Price RW. 1986. The AIDS dementia complex: II. Ann Neurol 19:525–535. https://doi.org/10.1002/ana.410190603.
6. Anthony IC, Ramage SN, Carnie FW, Simmonds P, Bell JE. 2005. Influence of HAART on HIV-related CNS disease and neuroinflammation. J Neuropathol Exp Neurol 64:529–536. https://doi.org/10.1093/jnen/64.6.529.
7. González-Scarano F, Martin-Garcia J. 2005. The neuropathogenesis of AIDS. Nat Rev Immunol 5:69–81. https://doi.org/10.1038/nri1527.
8. Cornford ME, Holden JK, Boyd MC, Berry K, Vinters HV. 1992. Neuropathology of the acquired immune deficiency syndrome (AIDS): report of 39 autopsies from Vancouver, British Columbia. Can J Neurol Sci 19:442–452. https://doi.org/10.1017/S0317167100041627.
9. Dambska M, Wisniewska K, Kozlowski P, Sher J. 1986. Neuropathology in acquired immune deficiency syndrome. Neuropatol Pol 24:133–143. (In Polish.)
10. Funata N, Maeda Y, Koike M, Okeda R. 1991. Neuropathology of the central nervous system in acquired immune deficiency syndrome (AIDS) in Japan. With special reference to human immunodeficiency virus-induced encephalomyelopathies. Acta Pathol Jpn 41:206–211. https://doi.org/10.1111/j.1440-1827.1991.tb01648.x.
11. Gray F, Gherardi R, Scaravilli F. 1988. The neuropathology of the acquired immune deficiency syndrome (AIDS). A review. Brain 111:245–266. https://doi.org/10.1093/brain/111.2.245.
12. Kato T, Hirano A, Llena JF, Dembitzer HM. 1987. Neuropathology of acquired immune deficiency syndrome (AIDS) in 53 autopsy cases with particular emphasis on microglial nodules and multinucleated giant cells. Acta Neuropathol 73:287–294. https://doi.org/10.1007/BF00686624.
13. Lang W, Miklossy J, Deruaz JP, Pizzolato GP, Probst A, Schaffner T, Gessaga E, Kleihues P. 1989. Neuropathology of the acquired immune deficiency syndrome (AIDS): a report of 135 consecutive autopsy cases from Switzerland. Acta Neuropathol 77:379–390. https://doi.org/10.1007/BF00687372.
14. Moskowitz LB, Hensley GT, Chan JC, Gregorios J, Conley FK. 1984. The neuropathology of acquired immune deficiency syndrome. Arch Pathol Lab Med 108:867–872.
15. Heaton RK, Clifford DB, Franklin DR, Woods SP, Ake C, Vaida F, Ellis RJ, Letendre SL, Marcotte TD, Atkinson JH, Rivera-Mindt M, Vigil OR, Taylor MJ, Collier AC, Marra CM, Gelman BB, McArthur JC, Morgello S, Simpson DM, McCutchan JA, Abramson I, Gamst A, Fennema-Notestine C, Jernigan TL, Wong J, Grant I, for the CHARTER Group. 2010. HIV-associated neurocognitive disorders persist in the era of potent antiretroviral therapy: CHARTER Study. Neurology 75:2087–2096. https://doi.org/10.1212/WNL.0b013e318200d727.
16. Eden A, Marcotte TD, Heaton RK, Nilsson S, Zetterberg H, Fuchs D, Franklin D, Price RW, Grant I, Letendre SL, Gisslén M. 2016. Increased intrathecal immune activation in virally suppressed HIV-1 infected patients with neurocognitive impairment. PLoS One 11:e0157160. https://doi.org/10.1371/journal.pone.0157160.
17. Zink MC, Suryanarayana K, Mankowski JL, Shen A, Piatak M, Spelman JP, Carter DL, Adams RJ, Lifson JD, Clements JE. 1999. High viral load in the cerebrospinal fluid and brain correlates with severity of simian immunodeficiency virus encephalitis. J Virol 73:10480–10488. https://doi.org/10.1128/JVI.73.12.10480-10488.1999.
18. Jin X, Bauer DE, Tuttleton SE, Lewin S, Gettie A, Blanchard J, Irwin CE, Safrit JT, Mittler J, Weinberger L, Kostrikis LG, Zhang L, Perelson AS, Ho DD. 1999. Dramatic rise in plasma viremia after $CD8^+$ T cell depletion in simian immunodeficiency virus-infected macaques. J Exp Med 189:991–998. https://doi.org/10.1084/jem.189.6.991.
19. Williams KC, Corey S, Westmoreland SV, Pauley D, Knight H, deBakker C, Alvarez X, Lackner AA. 2001. Perivascular macrophages are the primary cell type productively infected by simian immunodeficiency virus in the brains of macaques: implications for the neuropathogenesis of AIDS. J Exp Med 193:905–915. https://doi.org/10.1084/jem.193.8.905.
20. Ortiz AM, Klatt NR, Li B, Yi Y, Tabb B, Hao XP, Sternberg L, Lawson B, Carnathan PM, Cramer EM, Engram JC, Little DM, Ryzhova E, Gonzalez-Scarano F, Paiardini M, Ansari AA, Ratcliffe S, Else JG, Brenchley JM, Collman RG, Estes JD, Derdeyn CA, Silvestri G. 2011. Depletion of $CD4^+$ T cells abrogates post-peak decline of viremia in SIV-infected rhesus macaques. J Clin Invest 121:4433–4445. https://doi.org/10.1172/JCI46023.
21. Micci L, Alvarez X, Iriele RI, Ortiz AM, Ryan ES, McGary CS, Deleage C, McAtee BB, He T, Apetrei C, Easley K, Pahwa S, Collman RG, Derdeyn CA, Davenport MP, Estes JD, Silvestri G, Lackner AA, Paiardini M. 2014. CD4 depletion in SIV-infected macaques results in macrophage and microglia infection with rapid turnover of infected cells. PLoS Pathog 10:e1004467. https://doi.org/10.1371/journal.ppat.1004467.
22. Matsuda K, Riddick NE, Lee CA, Puryear SB, Wu F, Lafont BAP, Whitted S, Hirsch VM. 2017. A SIV molecular clone that targets the CNS and induces neuroAIDS in rhesus macaques. PLoS Pathog 13:e1006538. https://doi.org/10.1371/journal.ppat.1006538.
23. Calantone N, Wu F, Klase Z, Deleage C, Perkins M, Matsuda K, Thompson EA, Ortiz AM, Vinton CL, Ourmanov I, Loré K, Douek DC, Estes JD, Hirsch VM, Brenchley JM. 2014. Tissue myeloid cells in SIV-infected primates acquire viral DNA through phagocytosis of infected T cells. Immunity 41:493–502. https://doi.org/10.1016/j.immuni.2014.08.014.
24. Dang Q, Whitted S, Goeken RM, Brenchley JM, Matsuda K, Brown CR, Lafont BAP, Starost MF, Iyengar R, Plishka RJ, Buckler-White A, Hirsch VM. 2012. Development of neurological disease is associated with increased immune activation in simian immunodeficiency virus-infected macaques. J Virol 86:13795–13799. https://doi.org/10.1128/JVI.02174-12.
25. von Herrath M, Oldstone MB, Fox HS. 1995. Simian immunodeficiency virus (SIV)-specific CTL in cerebrospinal fluid and brains of SIV-infected rhesus macaques. J Immunol 154:5582–5589.
26. Hsu DC, Sunyakumthorn P, Wegner M, Schuetz A, Silsorn D, Estes JD, Deleage C, Tomusange K, Lakhashe SK, Ruprecht RM, Lombardini E, Im-Erbsin R, Kuncharin Y, Phuang-Ngern Y, Inthawong D, Chuenarom W, Burke R, Robb ML, Ndhlovu LC, Ananworanich J, Valcour V, O'Connell RJ, Spudich S, Michael NL, Vasan S. 2018. Central nervous system inflammation and infection during early, nonaccelerated simian-human immunodeficiency virus infection in rhesus macaques. J Virol 92:e00222-18. https://doi.org/10.1128/JVI.00222-18.

27. Irani DN, Griffin DE. 1996. Regulation of lymphocyte homing into the brain during viral encephalitis at various stages of infection. J Immunol 156:3850–3857.
28. Curis C, Percher F, Jeannin P, Montange T, Chevalier SA, Seilhean D, Cartier L, Couraud P-O, Gout O, Gessain A, Ceccaldi P-E, Afonso PV. 2016. Human T-lymphotropic virus type 1-induced overexpression of activated leukocyte cell adhesion molecule (ALCAM) facilitates trafficking of infected lymphocytes through the blood-brain barrier. J Virol 90:7303–7312. https://doi.org/10.1128/JVI.00539-16.
29. Shrestha B, Diamond MS. 2004. Role of $CD8^+$ T cells in control of West Nile virus infection. J Virol 78:8312–8321. https://doi.org/10.1128/JVI.78.15.8312-8321.2004.
30. McCandless EE, Zhang B, Diamond MS, Klein RS. 2008. CXCR4 antagonism increases T cell trafficking in the central nervous system and improves survival from West Nile virus encephalitis. Proc Natl Acad Sci U S A 105:11270–11275. https://doi.org/10.1073/pnas.0800898105.
31. Aloisi F, Pujol-Borrell R. 2006. Lymphoid neogenesis in chronic inflammatory diseases. Nat Rev Immunol 6:205–217. https://doi.org/10.1038/nri1786.
32. Mitsdoerffer M, Peters A. 2016. Tertiary lymphoid organs in central nervous system autoimmunity. Front Immunol 7:451.
33. Korin B, Ben-Shaanan TL, Schiller M, Dubovik T, Azulay-Debby H, Boshnak NT, Koren T, Rolls A. 2017. High-dimensional, single-cell characterization of the brain's immune compartment. Nat Neurosci 20:1300–1309. https://doi.org/10.1038/nn.4610.
34. Filipowicz AR, McGary CM, Holder GE, Lindgren AA, Johnson EM, Sugimoto C, Kuroda MJ, Kim W-K. 2016. Proliferation of perivascular macrophages contributes to the development of encephalitic lesions in HIV-infected humans and in SIV-infected macaques. Sci Rep 6:32900. https://doi.org/10.1038/srep32900.
35. Wu F, Ourmanov I, Kuwata T, Goeken R, Brown CR, Buckler-White A, Iyengar R, Plishka R, Aoki ST, Hirsch VM. 2012. Sequential evolution and escape from neutralization of simian immunodeficiency virus SIVsmE660 clones in rhesus macaques. J Virol 86:8835–8847. https://doi.org/10.1128/JVI.00923-12.
36. Wu F, Kirmaier A, Goeken R, Ourmanov I, Hall L, Morgan JS, Matsuda K, Buckler-White A, Tomioka K, Plishka R, Whitted S, Johnson W, Hirsch VM. 2013. TRIM5 alpha drives SIVsmm evolution in rhesus macaques. PLoS Pathog 9:e1003577. https://doi.org/10.1371/journal.ppat.1003577.
37. Wu F, Kirmaier A, White E, Ourmanov I, Whitted S, Matsuda K, Riddick N, Hall LR, Morgan JS, Plishka RJ, Buckler-White A, Johnson WE, Hirsch VM. 2016. TRIM5α resistance escape mutations in the capsid are transferable between simian immunodeficiency virus strains. J Virol 90:11087–11095. https://doi.org/10.1128/JVI.01620-16.
38. Matsuda K, Chen C-Y, Whitted S, Chertova E, Roser DJ, Wu F, Plishka RJ, Ourmanov I, Buckler-White A, Lifson JD, Strebel K, Hirsch VM. 2016. Enhanced antagonism of BST-2 by a neurovirulent SIV envelope. J Clin Invest 126:2295–2307. https://doi.org/10.1172/JCI83725.
39. Cardona AE, Huang D, Sasse ME, Ransohoff RM. 2006. Isolation of murine microglial cells for RNA analysis or flow cytometry. Nat Protoc 1:1947–1951. https://doi.org/10.1038/nprot.2006.327.